

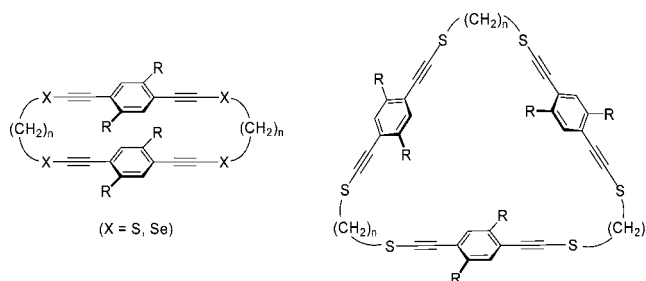
Macrocyclic Cyclophanes with Two and Three α,ω -Dichalcogena-1,4-diethynylaryl Units: Syntheses and Structural Properties

Daniel B. Werz,[†] Felix R. Fischer, Stefan C. Kornmayer, Frank Rominger, and Rolf Gleiter*

Organisch-Chemisches Institut der Universität Heidelberg, Im Neuenheimer Feld 270, D-69120 Heidelberg, Germany

rolf.gleiter@oci.uni-heidelberg.de

Received June 24, 2008



By means of four- and six-component cyclization reaction various cyclophanes were synthesized. The components were the di(lithium) salts of 1,4-di(ethynyl)benzene (**11**), 4,4'-di(ethynyl)biphenyl (**13**), 1,4-di(ethynyl)-2,5-di(*n*-hexyl)benzene (**18**), and 1,4-di(ethynyl)-2,5-di(*n*-propyl)benzene (**19**). These building blocks were reacted with α,ω -dithiocyanato-*n*-alkanes and α,ω -diselenocyanato-*n*-alkanes with $n = 3-6$. In the case of **10** also 1,1'-di(2-thiocyanatoethyl)cyclohexane (**24**) was reacted to afford a cyclophane comprising three subunits of **11**. From most of the resulting macrocyclic cyclophanes (**4**(*n*)) ($n = 3, 5$), **5**, **6**, **7**(*n*), **8**(*n*) ($n = 3-6$), **9**(*n*) ($n = 3, 5$), and **10**), we were able to grow single crystals. The X-ray analysis of **4**(**3**), **7**(**3**), **8**(**3**), **8**(**4**), **6**, **7**(**5**), and **8**(**5**) revealed close contacts between the chalcogen atoms. These chalcogen–chalcogen interactions impose a ribbon-shape arrangement of molecules in **4**(**3**) and a mutual crossing of two perpendicular planes built of **8**(**4**) molecules. For **4**(**3**) we found a close contact (3.28 Å) between the π planes of two neighboring C₆H₄ rings of different molecules, whereas in **8**(**4**) such a close contact (3.74 Å) was due to an intermolecular interaction. Tubular stacking of the macrocyclic rings was found for **7**(**5**) and **8**(**5**) caused by a ladder-type intermolecular chalcogen–chalcogen interaction.

Introduction

Cyclophanes (e.g., compounds of type **1**) are composed of planar aromatic rings which are tethered by aliphatic chains.¹ Thus the cyclophane ring system reveals the typical properties of both building units. Especially the topology of larger cyclophane rings provides a cavity prone to complex metal atoms and metal ions, respectively, or to host neutral molecules.

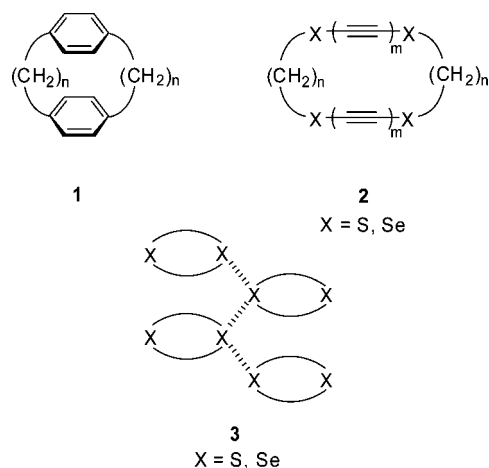
These properties are usually related to the π systems of cyclophanes, which act as electron donors or form weak hydrogen bonds with the guest molecules. Incidentally, the chemical behavior of the bridges has not been studied to the same extent as the aromatic building blocks. Here donor atoms such as nitrogen or chalcogen centers support the complexing properties of the cavity.²

[†] Present address: Institut für Organische und Biomolekulare Chemie der Georg-August-Universität Göttingen, Tammannstr. 2, D-37077 Göttingen, Germany.

(1) Reviews: (a) *Modern Cyclophane Chemistry*; Gleiter, R., Hopf, H., Eds.; Wiley-VCH: Weinheim, 2004. (b) Vögtle, F. *Cyclophane Chemistry*; Wiley-VCH: Chichester, 1993. (c) Diederich, F. *Cyclophanes*; Royal Society of Chemistry: Cambridge, 1991. (d) Kuhn, P. M.; Rosenfeld, S. M. *Cyclophanes*; Academic Press: New York, 1983; Vols. I and II.

(2) Reviews: (a) Gleiter, R.; Rausch, B. J.; Schaller, R. J. In *Modern Cyclophane Chemistry*; Gleiter, R.; Hopf, H., Eds.; Wiley-VCH: Weinheim, 2004, 159–188. (b) Schulz, J.; Vögtle, F. *Top. Curr. Chem.* **1994**, *172*, 41–86. (c) Mascal, M.; Kerdelhué, J. L.; Blake, A. J.; Cooke, P. A. *Angew. Chem.* **1999**, *111*, 2094–2096; *Angew. Chem., Int. Ed.* **1999**, *38*, 1968–1971. (d) Kunze, A.; Balalaie, S.; Gleiter, R.; Rominger, F. *Eur. J. Org. Chem.* **2006**, 2942–2955. (e) Kunze, A.; Gleiter, R.; Bethke, S.; Rominger, F. *Organometallics* **2006**, *25*, 4787–4791.

CHART 1



Recently, we have studied a number of monocyclic systems mirroring cyclophane topologies: rigid rods of two electron-rich alkyne units, placed opposite to each other, are tethered with two hydrocarbon chains of equal or nearly equal chain length (e.g., **2**).³ If the alkyne units were terminated with divalent chalcogen centers the cyclic systems formed tubular structures in the solid state. A closer investigation revealed that the tubes were formed by stacking of rings on top of each other.⁴ This high order in the solid state was caused by van der Waals forces between the chalcogen centers⁴ of various stacks as shown in **3** (Chart 1). Similar close contacts between two or more chalcogen atoms have been known for many years^{5–10} and have been identified by means of X-ray diffraction studies on single crystals or by solution NMR studies of carefully designed molecules. To interpret the short chalcogen–chalcogen distances, bonding models of different levels of sophistication were

(3) (a) Benisch, C.; Bethke, S.; Gleiter, R.; Oeser, T.; Pritzkow, H.; Rominger, F. *Eur. J. Org. Chem.* **2000**, 2479–2488. (b) Rausch, B. J.; Werz, D. B.; Ritinger, S.; Gleiter, R.; Oeser, T.; Rominger, F. *J. Chem. Soc., Perkin Trans. 2* **2002**, 72–76. (c) Werz, D. B.; Gleiter, R.; Rominger, F. *J. Org. Chem.* **2002**, 67, 4290–4297.

(4) (a) Werz, D. B.; Staeb, T. H.; Benisch, C.; Rausch, B. J.; Rominger, F.; Gleiter, R. *Org. Lett.* **2002**, 4, 339–342. (b) Werz, D. B.; Gleiter, R.; Rominger, F. *J. Am. Chem. Soc.* **2002**, 124, 10638–10639. (c) Gleiter, R.; Werz, D. B.; Rausch, B. J. *Chem. Eur. J.* **2003**, 9, 2676–2683. (d) Werz, D. B.; Rausch, B. J.; Gleiter, R. *Tetrahedron Lett.* **2002**, 43, 5767–5769. (e) Schulte, J. H.; Werz, D. B.; Rominger, F.; Gleiter, R. *Org. Biomol. Chem.* **2003**, 1, 2788–2794. (f) Werz, D. B.; Gleiter, R.; Rominger, F. *Organometallics* **2003**, 22, 843–849. (g) Werz, D. B.; Gleiter, R.; Rominger, F. *J. Org. Chem.* **2004**, 69, 2945–2952. (h) Werz, D. B.; Gleiter, R. *J. Org. Chem.* **2003**, 68, 9400–9405. (i) Benisch, C.; Werz, D. B.; Gleiter, R.; Rominger, F.; Oeser, T. *Eur. J. Inorg. Chem.* **2003**, 1099–1112. (j) Gleiter, R.; Werz, D. B. *Chem. Lett.* **2005**, 34, 126–131.

(5) (a) Glass, R. S.; Andruski, S. W.; Broeker, J. L.; Firouzabadi, H.; Steffen, L. K.; Wilson, G. S. *J. Am. Chem. Soc.* **1989**, 111, 4036–4045. (b) Glass, R. S.; Adamowicz, L.; Broeker, J. L. *J. Am. Chem. Soc.* **1991**, 113, 1065–1072. (c) Glass, R. S.; Andruski, S. W.; Broeker, J. L. *Rev. Heteroatom. Chem.* **1988**, 1, 31–45.

(6) (a) Fujihara, H.; Ishitani, H.; Takaguchi, Y.; Furukawa, N. *Chem. Lett.* **1995**, 24, 571–572. (b) Fujihara, H.; Yabe, M.; Chiu, J.-J.; Furukawa, N. *Tetrahedron Lett.* **1991**, 32, 4345–4348.

(7) (a) Hayashi, S.; Nakanishi, W. *J. Org. Chem.* **1999**, 64, 6688–6696. (b) Nakanishi, W.; Hayashi, S.; Toyota, S. *J. Org. Chem.* **1998**, 63, 8790–8800. (c) Nakanishi, W.; Hayashi, S.; Yamaguchi, H. *Chem. Lett.* **1996**, 25, 947–948.

(8) (a) Iwaoka, M.; Komatsu, H.; Katsuda, T.; Tomoda, S. *J. Am. Chem. Soc.* **2004**, 126, 5309–5317. (b) Tiecco, M.; Testaferri, L.; Santi, C.; Tomassini, C.; Santoro, S.; Marini, F.; Bagnoli, L.; Temperini, A.; Costantino, F. *Eur. J. Org. Chem.* **2006**, 4867–4873. (c) Iwaoka, M.; Takemoto, S.; Okada, M.; Tomoda, S. *Chem. Lett.* **2001**, 2, 132–133.

(9) (a) Barton, D. H. R.; Hall, M. B.; Lin, Z.; Parekh, S. I.; Reibenspies, J. *J. Am. Chem. Soc.* **1993**, 115, 5056–5059. (b) Fleischer, H.; Mitzel, N. W.; Schollmeyer, D. *Eur. J. Inorg. Chem.* **2003**, 5, 815–821.

(10) Gleiter, R.; Gyax, R. *Top. Curr. Chem.* **1976**, 63, 49–88, and references therein.

employed. In earlier days a donor–acceptor model was used,¹¹ which was refined on the basis of a one-electron model invoking the interaction of an occupied n(p)-type lone pair of a donor center and an empty σ^* orbital of a chalcogen–carbon bond.¹² In the case of three chalcogen atoms in close contact, their interaction was described as an electron-rich three-center bond.^{10,13} With the advent of more sophisticated quantum chemical methods these interactions have been modeled on the basis of semiempirical,¹⁴ HF-SCF,¹⁵ and DFT¹⁶ theory. However, recent studies have shown that for a quantitative description methods including electron correlation effects are necessary.^{17,18} To find out if further highly ordered structures in the solid state arise when the alkyne units are separated by aryl units we synthesized **4–10** and studied their structural properties.

The rather poor solubility of **4(3)**, **4(5)**, and **5** (Chart 2) in common organic solvents imposed difficulties regarding their purification. In an effort to overcome this problem we synthesized **6**, **7(3)–7(6)**, and **8(3)–8(6)** together with the side products **9(3)** and **9(5)** bearing alkyl substituents on the aromatic rings prone to increase the solubility. In the case of **10** we present an example where the alkyl groups were tethered to the bridge.

Results and Discussion

Syntheses. To derive the systems **4(3)** and **4(5)** we employed a four-component cyclization reaction of the di(lithium) salt of 1,4-di(ethynyl)benzene (**11**) and the corresponding α,ω -dithiocyanatoalkanes **12(n)** ($n = 3, 5$) following previously published procedures.^{3a,b,19} The dithiocyanatoalkanes used in this paper have been described in the literature.²⁰ The reaction was carried out in anhydrous THF under argon atmosphere at -40°C . The yields of the macrocyclization products were low and amounted to 7% for **4(3)** and 11% for **4(5)** (Scheme 1).

In analogy to **4(n)** the macrocycle **5** was obtained from 4,4'-di(ethynyl)biphenyl (**13**) and 1,5-dithiocyanatopentane (**12(5)**).²⁰ The yield of **5** was only 3%, and moreover the resulting cyclophane was nearly insoluble in any of the common solvents. NMR investigations had to be performed in hot toluene.

In an effort to increase the solubility of larger rings we attached alkyl groups to the aromatic moieties as depicted in **6–8** (Chart 2). As a starting material for **6** we first prepared 1,4-di(ethynyl)-2,5-di(*n*-hexyl)benzene (**18**) (Scheme 2).

(11) Bent, H. A. *Chem. Rev.* **1968**, 68, 587–648.

(12) (a) Rosenfield, R. E., Jr.; Dunitz, J. D. *J. Am. Chem. Soc.* **1977**, 99, 4860–4862. (b) Glusker, J. P. *Top. Curr. Chem.* **1998**, 198, 1–56. (c) Guru Row, T. N.; Parthasarathy, R. *J. Am. Chem. Soc.* **1981**, 103, 477–479. (d) Ramasubbu, N.; Parthasarathy, R. *Phosphorus, Sulfur, Silicon Relat. Elem.* **1987**, 31, 221–229.

(13) Gleiter, R.; Hoffmann, R. *Tetrahedron* **1968**, 24, 5899–5911.

(14) Boyd, D. B. *J. Phys. Chem.* **1978**, 82, 1407–1416.

(15) Angyan, J. G.; Poirier, R. A.; Kucsman, A.; Csizmadia, I. G. *J. Am. Chem. Soc.* **1987**, 109, 2237–2245.

(16) Sanz, P.; Yañez, M.; M6, O. *J. Phys. Chem. A* **2002**, 106, 4661–4668.

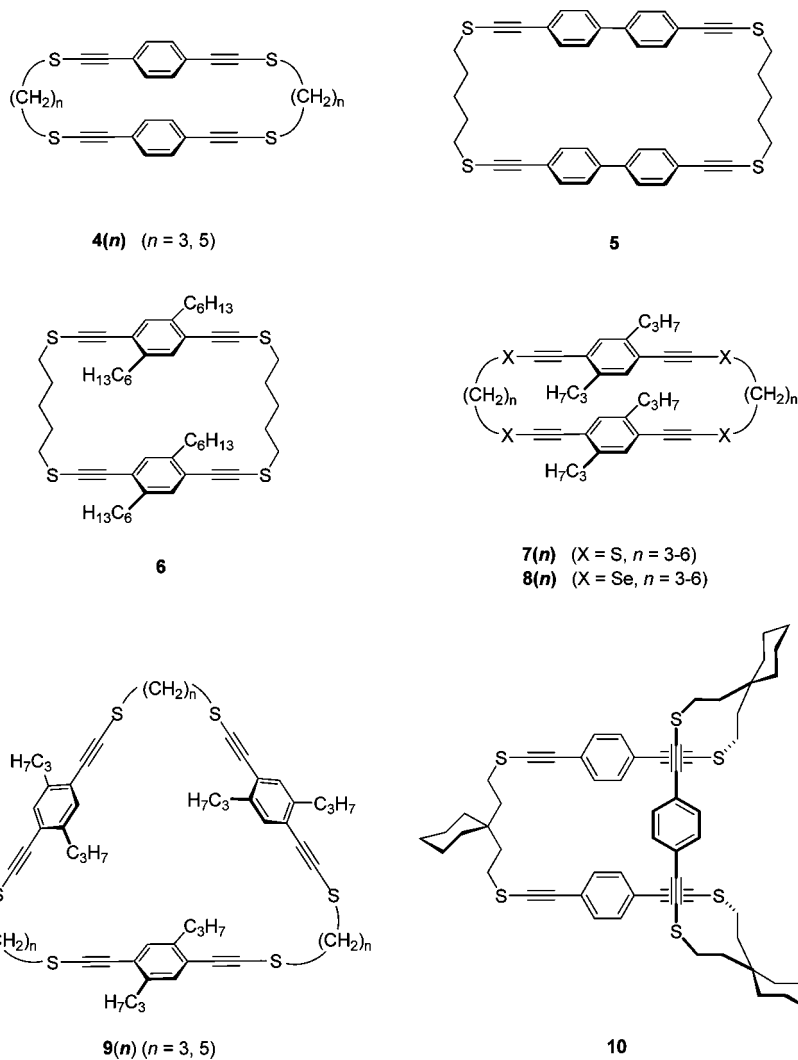
(17) (a) Whangbo, M.-H.; Novoa, J. J.; Jung, D.; Williams, J. M.; Kini, A. M.; Wang, H. H.; Geiser, U.; Beno, M. A.; Carlson, K. D. In *Organic Superconductivity*; Kresin, V. Z., Little, W. A., Eds.; Plenum Press: New York, 1990; pp 231–242. (b) Klinkhammer, K. W.; Pyykk6, P. *Inorg. Chem.* **1995**, 34, 4134–4138. (c) Pyykk6, P. *Chem. Rev.* **1997**, 97, 597–636.

(18) (a) Bleiholder, C.; Werz, D. B.; K6ppel, H.; Gleiter, R. *J. Am. Chem. Soc.* **2006**, 128, 2666–2674. (b) Bleiholder, C.; Gleiter, R.; Werz, D. B.; K6ppel, H. *Inorg. Chem.* **2007**, 46, 2249–2260.

(19) Brandsma, L. *Preparative Acetylene Chemistry*, 2nd ed.; Elsevier: Amsterdam, 1988; p 132.

(20) (a) Buff, H. L. *Liebig Ann. Chem.* **1856**, 100, 219–242. (b) Hagelberg, L. *Chem. Ber.* **1890**, 23, 1083–1092. (c) Braun, J.; Tr6mppler, A. *Chem. Ber.* **1910**, 43, 545–551. (d) v. Braun, J.; Lemke, G. *Chem. Ber.* **1922**, 55, 3536–3559.

CHART 2



Our synthesis of **18** commenced with 1,4-dichlorobenzene (**14**), which was reacted with 2 equiv of *n*-hexylbromide according to Kumada and Corriu²¹ to afford 1,4-di(*n*-hexyl)-benzene (**15**).²² To introduce the alkyne groups we first carried out an iodination²³ in the *ortho* positions of **15** to give **16**. Subsequent Sonogashira–Hagihara coupling²⁴ with trimethylsilylethyne (TMSA) provided **17**. The deprotection of **17** with diluted NaOH yielded the unprotected aromatic diyne **18**. With **18** at hand we performed a four-component cyclization reaction using 2 equiv of 1,5-dithiocyanatopentane (**12(5)**) and 2 equiv of **18** analogous to the synthesis of **4(5)** (Scheme 1). The yield of the desired macrocycle **6** amounted to 8%.

The preparations of **7(n)** and **8(n)** were carried out in accordance to that of **6**. The starting materials were 1,4-di(ethynyl)-2,5-di(*n*-propyl)benzene (**19**) and the α,ω -dithiocyanatoalkanes **12(3)**–**12(6)**²⁰ as well as the α,ω -diselenocyanatoalkanes **20(3)**–**20(6)**.²⁵ The yields of the cyclophanes **7(n)** ($n = 3-6$) and **8(n)** ($n = 3-6$) varied between 3% (**8(4)**) and

17% (**7(3)**). During the preparation of **7(3)** and **7(5)** we also isolated the corresponding hexathiamacrocycles **9(3)** and **9(5)** as colorless oils in low yields (Scheme 3).

The investigations of the molecular structures of **6**–**8** revealed that the alkyl groups attached to the aromatic rings prevent the inclusions of solvent molecules in the interior of the cyclophanes due to the tilt of the benzene rings around the S...S axis (see below). Therefore we looked for simple ways of attaching solubilizing functional groups to the alkyl bridges of the cyclophanes. In a first attempt we replaced the central CH₂ group of a pentamethylene chain by a 1,1-diethylcyclohexane moiety. The starting material 3,3-pentamethyleneglutaric acid (**21**) (Scheme 4) is commercially available. Scheme 4 summarizes a straightforward protocol to synthesize the 1,1-di(2-chalcogenocyanatoethyl)cyclohexanes **24** and **25**. The diacid **21** was reduced using LiAlH₄ to afford the 1,5-diol **22**.³⁰ The latter was converted to **24** and **25** via the 1,1'-di(2-methanesulfonyloxyethyl)cyclohexane (**23**) in an overall yield of ca. 60%.

The reaction of the di(lithium) salt of **11** with **24** afforded the cyclophane **10** in only <1% yield (Scheme 5). The expected

(21) (a) Tamao, K.; Sumitani, S.; Kumada, M. *J. Am. Chem. Soc.* **1972**, *94*, 4374–4376. (b) Corriu, R. J. P.; Masse, J. P. *J. Chem. Soc., Chem. Commun.* **1972**, 144.

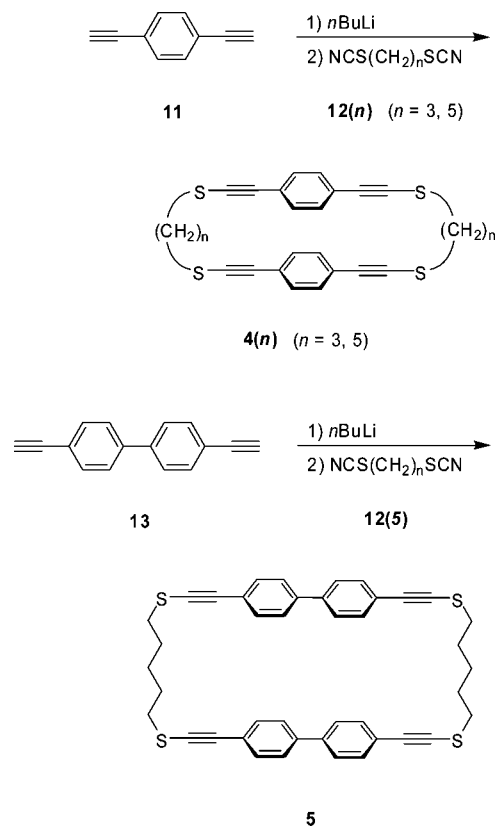
(22) Rehahn, H.; Schlüter, A.-D.; Feast, W. J. *Synthesis* **1988**, 386–388.

(23) Kukula, H.; Veit, S.; Godt, A. *Eur. J. Org. Chem.* **1999**, 277–286.

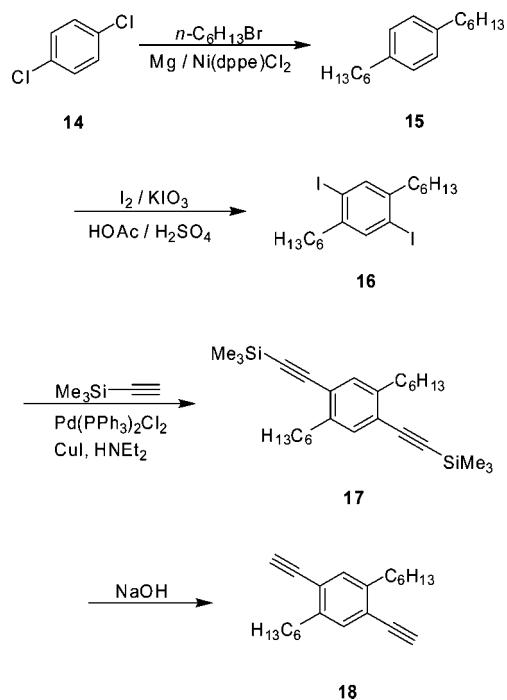
(24) Takahashi, S.; Kuroyama, Y.; Sonogashira, K.; Hagihara, N. *Synthesis* **1980**, 627–630.

(25) (a) Goodall, D. C. *J. Inorg. Nucl. Chem.* **1968**, *30*, 1269–1270. (b) Clarebeau, M.; Cravador, A.; Dumont, W.; Hevesi, L.; Krief, A.; Lucchetti, J.; van Ende, D. *Tetrahedron* **1985**, *41*, 4793–4812. (c) Krief, A.; Delmotte, C.; Dumont, W. *Tetrahedron* **1997**, *53*, 12147–12158.

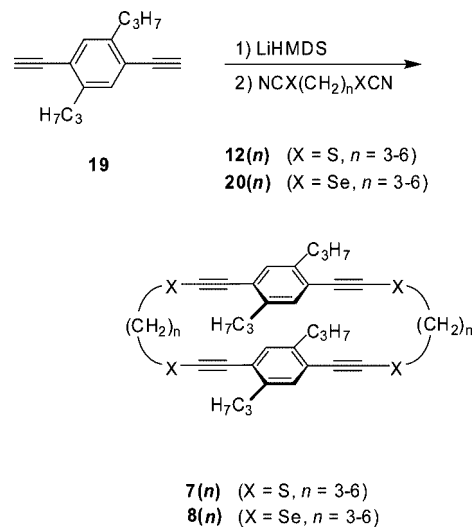
SCHEME 1



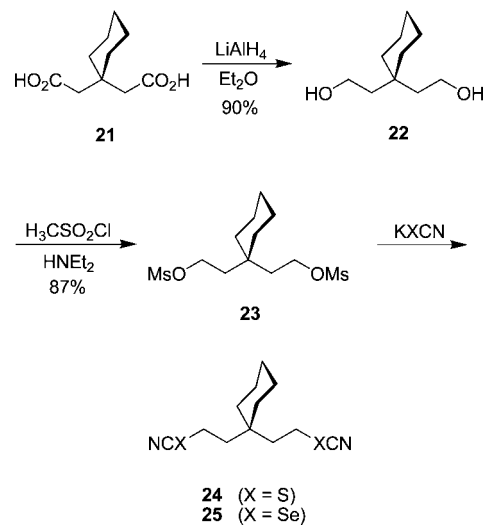
SCHEME 2



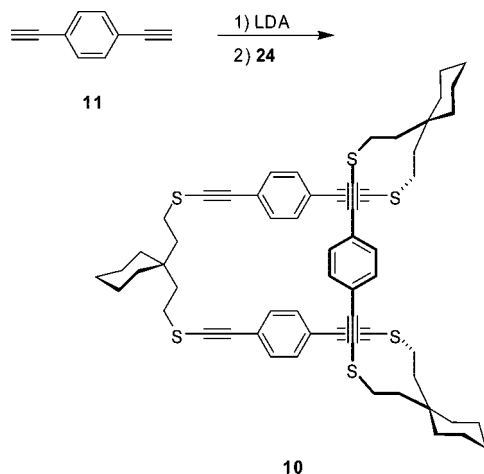
SCHEME 3



SCHEME 4



SCHEME 5

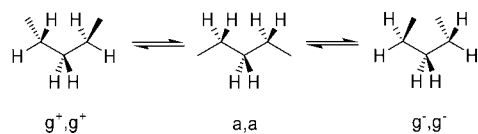


product resulting from a four-component cyclization of 2 equiv of **11** and **24** could not be detected. We attribute this observation to the fact that the sterically demanding six-membered ring in the center of the pentano chains in **10** is only able to adopt the *exo*-position if the pentano chain chooses a *gauche-gauche* (*g,g*)[±] conformation instead of the *anti,anti* (*a,a*) conformation depicted in Scheme 6.²⁶ The assumption of a *gauche-gauche*

(*g,g*)[±] conformation of the pentano chains in **10** is supported by the molecular structures of **24** and **25** (Figure 1).

Structural Investigations. We were able to grow single crystals of **4(3)**, **4(5)**, **6**, **7(3)**–**7(5)**, and **8(3)**–**8(6)**, which were suited for X-ray diffraction experiments. We have subdivided

SCHEME 6



the structures with respect to the chain lengths which connect the α, ω -dichalcogeno(1,4-diethynylbenzene) units.

Rings with Propylene Bridges. The only structure in all measured species without any crystallographically imposed symmetry is that of **4(3)**. One propylene chain adopts a zigzag conformation including the terminal sulfur atoms, the other shows a gauche conformation at the end with the sulfur center S3 (Figure 2). The sulfur centers are involved in single (S2, S3) or double (S4) close $S \cdots S$ contacts (3.336 and 3.907 Å that combine four cyclophanes into one unit. As a result a ribbon of molecules is created (Figure 2). Within this assembly we encounter for each pair of molecules two parallel phenyl rings

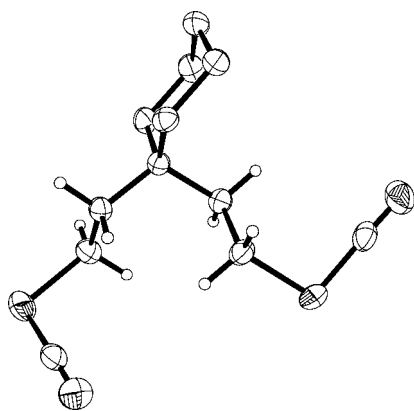


FIGURE 1. ORTEP plot (50% ellipsoid probability) of the molecular structure of **24**. Hydrogen atoms of the cyclohexyl part are omitted for the sake of clarity.

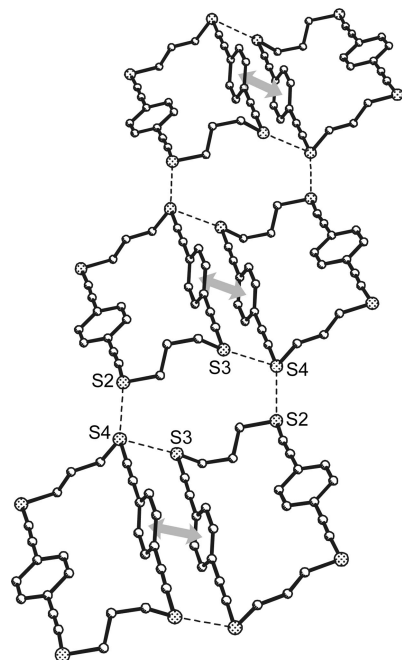


FIGURE 2. Structure of **4(3)** in the solid state oriented into a ribbon via short $S \cdots S$ interactions. Hydrogen atoms are omitted for the sake of clarity.

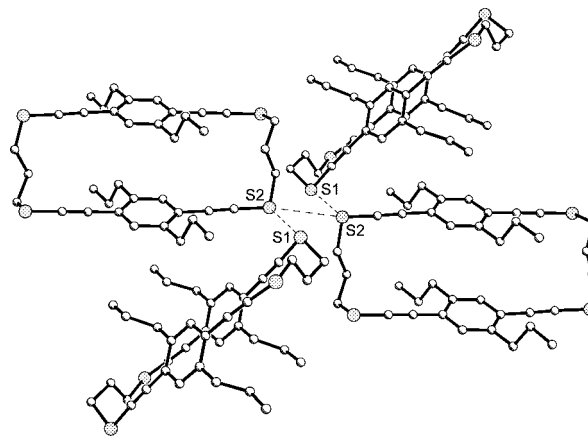


FIGURE 3. Chalcogen–chalcogen network between S1 and S2 centers of **7(3)**. Hydrogen atoms are omitted for the sake of clarity.

with a very close π – π distance of 3.28 Å. (In Figure 2 this overlap is indicated by a gray arrow.)

This distance is shorter than the interlayer spacing in graphite (3.345 Å)²⁷ or the interplanar distance of 2,7-dimethylpyrene (3.45 Å).²⁸ The π – π interaction in **4(3)** is facilitated by a rotation of one aromatic ring of each cyclophane by 55.8° with respect to the ring plane defined by the intramolecular vector between the centers of the aromatic units. The related thia- and selenamacrocycles bearing propyl substituents on the aromatic rings (**7(3)**, **8(3)**) show different features. Although both structures are alike but not isomorphic they reveal very similar crystal structures. The molecules adopt a conformation with inversion symmetry in the crystal. The propylene chains show a gauche conformation at the S1 end. The chalcogen atoms among neighboring molecules show close contacts between S1 \cdots S2 \cdots S2 \cdots S1 (Se1 \cdots Se2 \cdots Se2 \cdots Se1, respectively) centers (Figure 3) providing for a two-dimensional chalcogen network between layers of cycles. The distances between the proximal chalcogen centers are in the case of the sulfur congener 3.575, 3.624, and 3.575 Å and in the case of the selenium congener 3.693, 3.583, and 3.693 Å.

Rings with Butylene Bridges. The molecular structure of **7(4)** is based on an inversion symmetry with *gauche* conformations of both sulfur atoms at the end of the butylene chains. In the crystal packing no stacking or close $S \cdots S$ contacts were found. For **8(4)** we observed a rather complex structure in the solid state which will be described in a stepwise fashion. As previously mentioned in the case of **7(4)** the butylene chains in **8(4)** adopt a *gauche* conformation at the selenium ends. In contrast to all other ring systems in the series with inversion symmetry, the conformation of the molecule comprises a 2-fold symmetry axis (Figure 4a). This leads to a close (3.74 Å), eclipsed stacking of the two aromatic rings, with a cross-over of the rigid alkyne units. Via short Se \cdots Se contacts (3.697 Å) the molecules are connected to sets of parallel grid-like planes, as shown in Figure 4b. This figure also depicts the eclipsed stacking with complete overlap of the benzene rings. The structure of **8(4)** in the solid state can be described as two perpendicular oriented equivalent planes (Figure 4c). The mutual crossing of the two planes occurs through the meshes of the grid without building contacts between the perpendicular sets of planes.

Rings with Pentylene Bridges. This group of molecules comprises the macrocycles **4(5)**, **6**, **7(5)**, and **8(5)**. The unsubstituted cyclophane **4(5)** reveals a centrosymmetric structure with

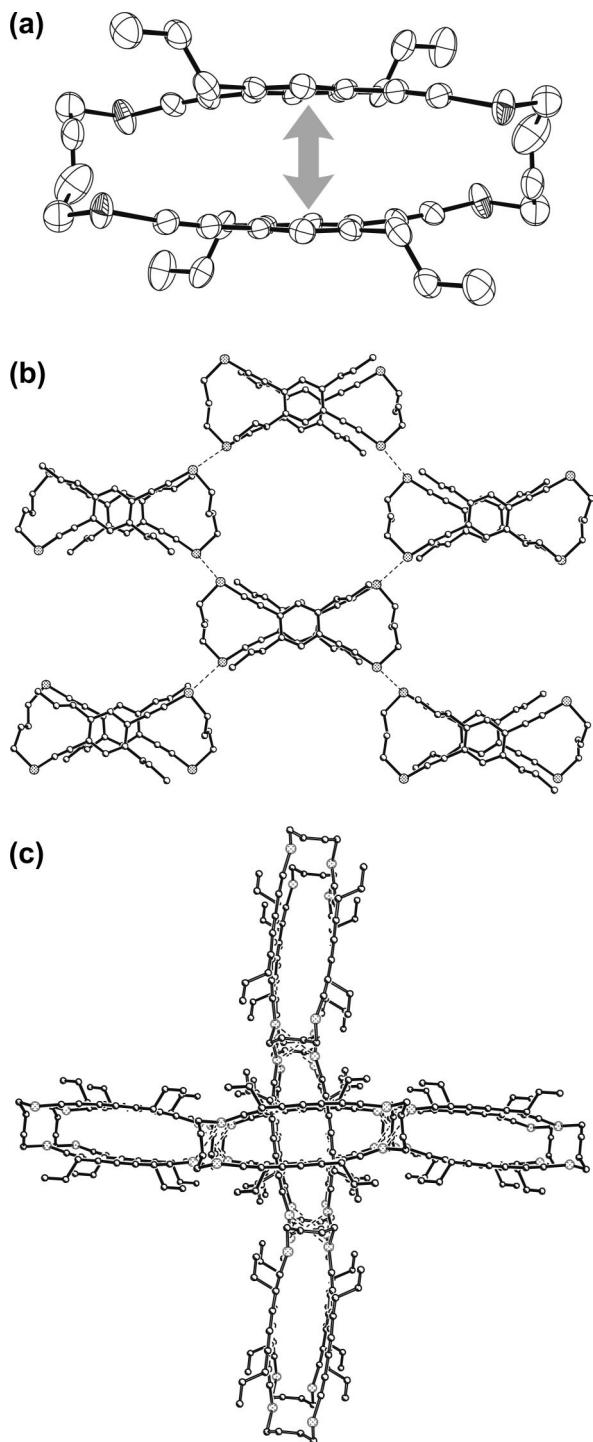


FIGURE 4. (a) ORTEP plot (50% ellipsoid probability) of the molecular structure of **8(4)** showing a π - π interaction between the phenyl rings, which are stacked in an eclipsed conformation on top of each other (see also panel b). Hydrogen atoms are omitted for the sake of clarity. (b) One plane of **8(4)** molecules in the solid state. The short Se \cdots Se interactions are indicated by dots. Hydrogen atoms are omitted for the sake of clarity. (c) Mutual intercrossing of two perpendicular planes of **8(4)** molecules in the solid state. Hydrogen atoms are omitted for the sake of clarity.

a clean zigzag conformation in both methylene chains, including the terminal sulfur atoms. In the crystal neither stacking of the molecules nor intermolecular S \cdots S contacts were observed. We cannot rule out weak sulfur- π interactions between the S atoms and the aromatic rings since the contact (3.688–3.709 Å) is

TABLE 1. List of Adopted Conformations and Torsion Angles [deg] of **4(3)**, **7(3)**, **8(3)**, **7(4)**, **8(4)**, **4(5)**, **6**, **7(5)**, **8(5)**, and **8(6)**^a

spacer length	compound	chalcogen	torsion angle α	conformation ^c	torsion angle β
3	4(3) ^b	S	24.0	a	1.3
			9.3	a	
			59.2	g	55.8
			19.0	a	
			19.4	g	41.2
	7(3)	S	32.4	a	
			47.3	g	44.2
4	7(4)	S	27.7	g	57.7
			26.6	g	
			13.1	g	86.8
			10.1	g	
			85.6	a	64.9
	4(5)	S	39.3	a	
			29.6	g	31.5
5	6	S	24.5	a	
			21.6	g	60.3
			37.9	g	
			21.5	g	59.9
			39.8	g	
	8(5)	Se	5.5	a	11.5
			1.3	a	

^a For the definition of α and β see Figure 7. ^b Two independent molecules exist in the unit cell. ^c a = *anti*; g = *gauche*.

only slightly longer than the sum of the van der Waals radii of benzene and sulfur (3.55 Å).²⁹

The congener with two hexyl substituents at the aromatic rings (**6**) is centrosymmetric as is **4(5)**, yet it shows one sulfur atom (S1) per chain with *gauche* conformation with respect to the pentylene spacer (Figure 5, left). The crystal packing of **6** is dominated by the parallel orientation of the dihexyl substituted aromatic rings. It provides for only one S \cdots S contact (S1 \cdots S1 = 3.669 Å). In Figure 5, left, we have compared the molecular structures of **4(5)** (open bonds) with no *gauche* conformation with that of **6** (black solid bonds) with one *gauche* conformation. The transformation of the skeleton of **4(5)** into that of **6** is indicated by the gray arrows.

With propyl substituents at the aromatic rings we encounter two isomorphous crystallizing sulfur-, **7(5)**, and selenium-containing, **8(5)**, compounds. In both molecules the two chalcogen atoms of each chain adopt a *gauche* conformation with respect to the pentamethylene spacers.

In Figure 5, right, we have compared **6** with one *gauche* conformation (black solid bond) with **7(5)** (black broken bonds). The adaptation of the second *gauche* conformation in going from **6** to **7(5)** is indicated by a gray arrow. It is interesting to note that the switch from **6** to **7(5)** hardly deforms the other parts of the ring.

The two *gauche* conformations of the chalcogen atoms in **7(5)** and **8(5)** allow a rather weak interaction between the chalcogen centers (S \cdots S = 4.089 Å, Se \cdots Se = 4.015 Å) giving rise to a ladder-like motif^{3,4} with stacked molecules as shown in Figure 6.

(26) (a) Eliel, E. L.; Wilen, S. H.; Mander, L. N. *Stereochemistry of Organic Compounds*; J. Wiley & Sons: New York, 1994; p 603. (b) Dale, J. *Stereochemistry and Conformation Analysis*; Verlag Chemie: New York, 1978.

(27) Franklin, R. E. *Acta Crystallogr.* **1951**, *4*, 253–261.

(28) Irgartinger, H.; Kirrstetter, R. G. H.; Krieger, C.; Rodewald, H.; Staab, H. A. *Tetrahedron Lett.* **1977**, *18*, 1425–1428.

(29) Pauling, L. *The Nature of the Chemical Bond*, 3rd ed.; Cornell University Press: Ithaca, NY, 1973.

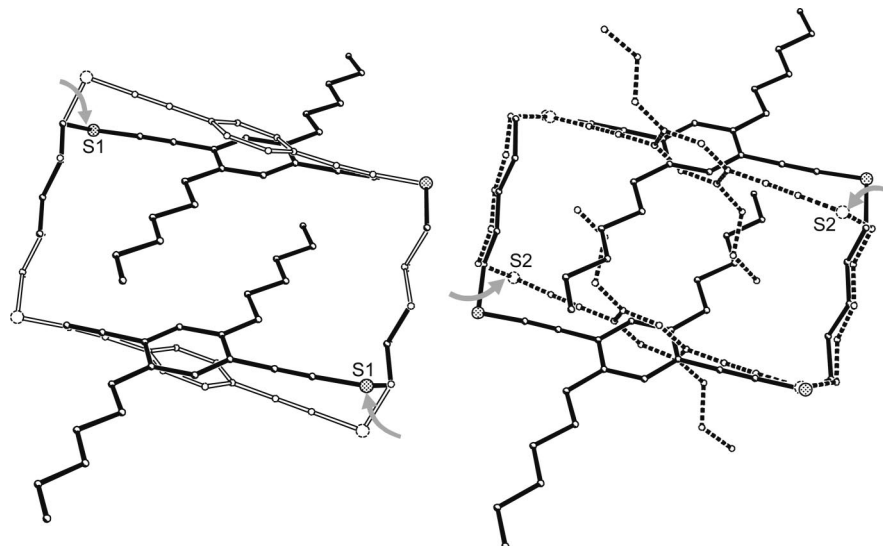


FIGURE 5. (Left) Comparison of the ring size of **4(5)** without *gauche* conformation (open bonds) with **6** with one *gauche* conformation in each bridge (solid bonds) demonstrating the ring size as a function of conformation. Hydrogen atoms are omitted for the sake of clarity. (Right) Comparison of **6** and **7(5)** with one and two *gauche* conformations, respectively, in the chains. The shape of **7(5)** is indicated in black broken lines. Hydrogen atoms are omitted for the sake of clarity.

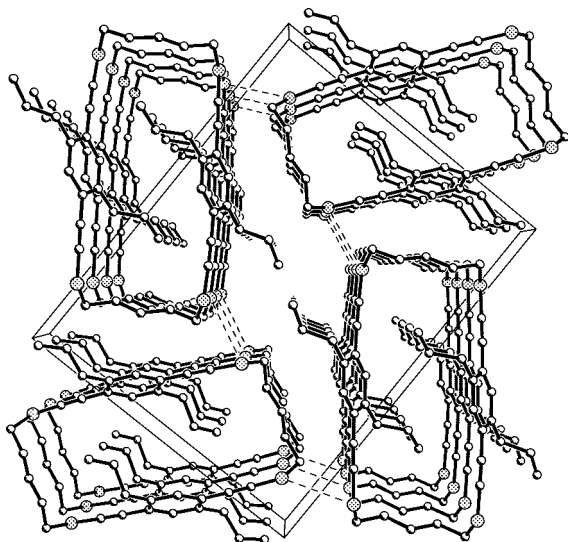


FIGURE 6. Stacking of the rings of **8(5)** in the solid state. The intermolecular ladder-type interaction between the chalcogen centers is indicated by broken lines. Hydrogen atoms are omitted for the sake of clarity.

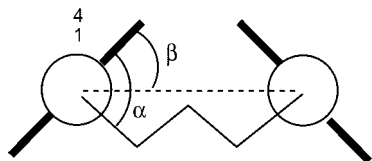


FIGURE 7. Definition of the torsional angles α and β on hand of a Newman projection of **4(3)**.

Rings with Hexylene Bridges. The largest spacers in this series were employed in the synthesis of **8(6)**. Again the solid state structure shows inversion symmetry. The *zigzag* conformation of the hexylene chains without any *gauche* conformation of the terminal selenium atoms opens a very wide ring, providing

TABLE 2. Recorded van der Waals Distances [\AA] of Chalcogen Centers X (X = S or Se) in **4(3)**, **7(3)**, **8(3)**, **8(4)**, **6**, **7(5)**, and **8(5)**

compound	X...X	\AA
4(3)	S4...S2	3.336
	S4...S3	3.907
7(3)	S2...S1	3.575
	S2...S2	3.624
8(3)	Se2...Se1	3.693
	Se2...Se2	3.583
8(4)	Se1...Se1	3.697
6	S1...S1	3.669
7(5)	S1...S2	4.089
8(5)	Se1...Se2	4.015

for an orientation of the aromatic rings in the plane of the macrocycle. No stacking or short Se...Se contacts were observed.

A comparison of the structural parameters of **4(3)**, **7(3)**, **8(3)**, **7(4)**, **8(4)**, **4(5)**, **6**, **7(5)**, **8(5)**, and **8(6)** (Table 1) reveals very similar bond distances in all rings. The average value for the distance between the aromatic rings and the triple bonds amounts to 1.44 \AA , the length of the triple bonds was found to be 1.20 \AA , and the average bond length between the triple bonds and the sulfur (selenium) atoms amounts to 1.69 (1.83) \AA . More variation is found for the torsion angles α and β (see Figure 7). The angle α is defined as the torsion of the S(e)–CH₂ bond with respect to the aromatic plane. The angle β measures the rotation of the aromatic ring with respect to a line going through centers 1 and 4 of each aromatic ring. No obvious and general correlation between the different torsion angles and the conformation (*anti* or *gauche*) can be found. The distribution of α shows a pattern with a maximum between 10° and 30° and a minimum close to 90°. However, quantum chemical calculations performed at the B3LYP/6-31G(d) level of theory did not reveal any significantly favored conformation for the model system PhCCXMe (X = S, Se).

At several occasions we noticed short contacts between the chalcogen centers. This is documented in Figures 2, 3, 4b, and 6. Table 2 summarizes the recorded values. It is found that the

TABLE 3. Crystal Data and Details of the Refinement Procedure for **4(3)**, **4(5)**, **6**, **7(3)**, **7(4)**, and **7(5)**

	4(3)	4(5)	6	7(3)	7(4)	7(5)
empirical formula	C ₃₃ H ₂₈ S ₄	C ₃₀ H ₂₈ S ₄	C ₅₄ H ₇₆ S ₄	C ₃₈ H ₄₄ S ₄	C ₄₀ H ₄₈ S ₄	C ₄₂ H ₅₂ S ₄
formula weight	552.84	516.80	853.44	628.97	657.02	685.08
crystal system	triclinic	monoclinic	triclinic	monoclinic	monoclinic	monoclinic
space group	<i>P</i> $\bar{1}$	<i>P</i> 2 ₁ / <i>c</i>	<i>P</i> $\bar{1}$	<i>P</i> 2 ₁ / <i>c</i>	<i>P</i> 2 ₁ / <i>c</i>	<i>P</i> 2 ₁ / <i>n</i>
<i>a</i> [Å]	9.8227(2)	11.3467(3)	8.2206(3)	13.159(2)	9.6400(2)	5.9995(1)
<i>b</i> [Å]	10.8655(2)	10.1243(3)	12.8156(4)	9.170(1)	17.2157(1)	20.0529(3)
<i>c</i> [Å]	13.7005(2)	12.5302(3)	13.7297(5)	15.565(2)	11.4959(2)	16.1288(2)
α [deg]	90.428(1)	90	65.421(1)	90	90	90
β [deg]	96.336(1)	92.643(1)	86.628(2)	114.261(3)	106.265(1)	95.919(1)
γ [deg]	93.668(1)	90	75.320(1)	90	90	90
<i>Z</i>	2	2	1	2	2	2
<i>V</i> [Å ³]	659.01(3)	1437.91(7)	1270.66(8)	1712.3(4)	1831.49(5)	1930.07(5)
<i>D</i> _{calc} [g/cm ³]	1.27	1.19	1.12	1.22	1.19	1.18
μ [mm ⁻¹]	0.35	0.35	0.22	0.30	0.29	0.27
max/min transm	0.97/0.87	0.96/0.72	0.97/0.91	0.97/0.93	0.94/0.88	0.96/0.90
θ range (deg)	1.50 – 27.47	1.80 – 27.46	1.63 – 27.50	2.6 – 28.3	2.2 – 26.4	1.6 – 26.4
reflections collected	14927	14384	13289	17081	15793	17828
independent/ <i>R</i> _{int}	6594 (0.029)	3286 (0.035)	5785 (0.048)	4212 (0.036)	3732 (0.029)	3958 (0.036)
observed (<i>I</i> > 2 σ (<i>I</i>))	4671	2534	2827	3819	2836	3033
goodness-of-fit on <i>F</i> ²	1.01	1.03	0.98	1.21	1.05	1.04
<i>R</i> (<i>F</i>)	0.037	0.041	0.055	0.049	0.037	0.035
<i>R</i> _w (<i>F</i> ²)	0.085	0.103	0.130	0.115	0.089	0.078
$\Delta\rho$ max/min (eÅ ⁻³)	0.35/–0.27	0.47/–0.38	0.32/–0.23	0.52/–0.25	0.24/–0.21	0.24/–0.30

TABLE 4. Crystal Data and Details of the Refinement Procedure for **8(3)**, **8(4)**, **8(5)**, **8(6)**, **24**, and **25**

	8(3)	8(4)	8(5)	8(6)	24	25
empirical formula	C ₃₈ H ₄₄ Se ₄	C ₄₆ H ₅₄ Se ₄	C ₄₂ H ₅₂ Se ₄	C ₄₄ H ₅₆ Se ₄	C ₁₂ H ₁₈ N ₂ S ₂	C ₁₂ H ₁₈ N ₂ Se ₂
formula weight	816.57	922.73	872.68	900.73	254.40	348.20
crystal system	monoclinic	tetragonal	monoclinic	monoclinic	monoclinic	monoclinic
space group	<i>P</i> 2 ₁ / <i>c</i>	<i>P</i> 4 ₂ / <i>c</i>	<i>P</i> 2 ₁ / <i>n</i>	<i>P</i> 2 ₁ / <i>c</i>	<i>P</i> 2 ₁ / <i>c</i>	<i>P</i> 2 ₁ / <i>c</i>
<i>a</i> [Å]	12.5412(3)	17.2898(3)	5.9637(6)	12.646(1)	11.6618(4)	11.646(1)
<i>b</i> [Å]	8.8176(2)	17.2898(3)	19.835(2)	10.267(1)	10.3412(4)	10.434(1)
<i>c</i> [Å]	16.9559(4)	14.4921(4)	16.5139(17)	17.521(2)	11.5186(4)	11.443(1)
α [deg]	90	90	90	90	90	90
β [deg]	110.527(1)	90	95.294(2)	106.627(3)	107.935(1)	106.003(2)
γ [deg]	90	90	90	90	90	90
<i>Z</i>	2	4	2	2	4	4
<i>V</i> [Å ³]	1755.99(7)	4332.23(16)	1945.1(3)	2179.7(4)	1321.61(8)	1336.8(2)
<i>D</i> _{calc} [g/cm ³]	1.54	1.41	1.49	1.37	1.28	1.73
μ [mm ⁻¹]	4.20	3.42	3.80	3.39	0.38	5.51
max/min transm	0.46/0.28	0.82/0.55	0.68/0.64	0.69/0.20	0.96/0.91	0.73/0.56
θ range (deg)	1.7 – 27.5	1.7 – 27.8	2.40 – 28.32	2.33 – 20.81	1.84 – 27.48	1.82 – 28.31
reflections collected	17656	44476	19785	11141	13354	13812
independent/ <i>R</i> _{int}	4006/0.028	5082/0.144	4801/0.036	2251/0.043	3022/0.032	3322/0.021
observed (<i>I</i> > 2 σ (<i>I</i>))	3258	2611	4103	1895	2470	2991
goodness-of-fit on <i>F</i> ²	1.06	1.01	1.05	1.03	1.04	1.07
<i>R</i> (<i>F</i>)	0.025	0.041	0.027	0.031	0.032	0.040
<i>R</i> _w (<i>F</i> ²)	0.057	0.066	0.057	0.074	0.075	0.093
$\Delta\rho$ max/min (eÅ ⁻³)	0.48/–0.62	0.43/–0.67	0.59/–0.28	0.45/–0.43	0.26/–0.25	1.18/–0.26

distances recorded for the S \cdots S contacts are slightly below or close to the sum of the van der Waals radii (3.70 Å).²⁹ The same holds true for the Se \cdots Se distances where the sum of the van der Waals radii is 4.00 Å.²⁹ The anticipated tubular structures were only found in the cases of **7(5)** and **8(5)** (c.f. Figure 6).

Conclusion

In the past years we prepared and investigated macrocyclic rings composed of two or three rigid units and two or three flexible bridges comprising four to six chalcogen atoms at the termini of the rigid subunits (e.g., **2**, Chart 1). Intermolecular van der Waals forces between chalcogen centers gave rise to tubular structures (e.g., **3**, Chart 1). Herein we describe the synthesis and the structural variations induced by using α,ω -dichalcogena(1,4-diethynylbenzene) units (**4**) and α,ω -dichalcogena(1,4-diethynylbiphenyl) units (**5**) as building

blocks. Initial problems caused by the low solubility of the macrocycles **4** and **5** were overcome by the introduction of solubilizing alkyl chains on the aromatic rings of macrocycles **6–8**. X-ray crystal structure analysis revealed the formation of tubular structures in the case of the cyclophanes **7(5)** and **8(5)**. The study of chalcogen–chalcogen interactions led to the identification of particularly well-defined solid-state architectures: **4(3)** crystallizes in a ribbon structure comprising close π – π interactions between neighboring aromatic rings. In the case of **8(4)** we identified eclipsed intramolecular aromatic π – π stacking interactions. The short intermolecular Se \cdots Se interaction in **8(4)** gave rise to two-dimensional sheets crossing each other mutually in a perpendicular way. Despite the very similar scaffolds of **4(n)–7(n)** we observe a great variety of their solid state structures. This observation was traced back to a subtle interplay between weak forces among the chalcogen centers and π – π interactions of the

aromatic units on one side and steric effects within and between alkyl chains and groups, respectively, on the other.

Experimental Section

General Procedure for the Preparation of Tetrathia- and Tetraselenamacrocycles 4(*n*), 5, 6, 7(*n*), and 8(*n*). A flame-dried 250-mL Schlenk tube was charged under argon with 1.0 equiv of 1,4-di(ethynyl)-2,5-di(*n*-propyl)benzene in 200 mL of anhydrous THF and cooled to $-40\text{ }^{\circ}\text{C}$. Then, 2.0 equiv of *n*-butyllithium (*n*BuLi) or lithium hexamethyldisilazide (LiHMDS) in THF was slowly added, and the resulting suspension was vigorously stirred for 15 min at $-40\text{ }^{\circ}\text{C}$. A flame-dried 2000-mL round-bottom flask with two 250-mL addition funnels was charged under argon with 750 mL of anhydrous THF and cooled to $-50\text{ }^{\circ}\text{C}$. The above prepared solution of the lithium salt was transferred into the first funnel and diluted with dry THF to a total volume of 250 mL. The second funnel was charged with 1.0 equiv of α,ω -dithiocyanatoalkane or α,ω -diselenocyanatoalkane in 250 mL of anhydrous THF. Both solutions were added simultaneously at $-50\text{ }^{\circ}\text{C}$ over a period of 4–5 h. The resulting solution was stirred for 12 h at $24\text{ }^{\circ}\text{C}$, and the solvent was concentrated by rotary evaporation. The residue was filtered through a plug of silica (SiO_2 ; 3% NEt_3 , toluene). Column chromatography (SiO_2 ; 3% NEt_3 , hexane/toluene) of the crude product yielded the macrocycles as colorless solids. Representative analytical data are given below.

4,8,14,18-Tetrathia-1²,1⁵,11²,11⁵-tetra(*n*-propyl)-1(1,4),11(1,4)-dibenzenacycloeicosa-2,9,12,19-tetraynophane (7(3)). Starting materials: 1,4-di(ethynyl)-2,5-di(*n*-propyl)benzene (**19**, 2.08 g, 9.9 mmol), LiHMDS (1.06 M in THF, 19.0 mL, 20.1 mmol), 1,3-dithiocyanatopropane (**12(3)**, 1.57 g, 9.9 mmol). Column chromatography (SiO_2 ; 3% NEt_3 , hexane/toluene, 3:1). Yield: 534 mg (17%) of **7(3)** as a colorless solid. R_f (SiO_2 , hexane/toluene, 3:1) 0.26; mp $158\text{ }^{\circ}\text{C}$; $^1\text{H NMR}$ (500 MHz, CD_2Cl_2) δ 6.89 (s, 4 H), 2.82 (t, $^3J = 7.4\text{ Hz}$, 8 H), 2.44 (quint., $^3J = 7.3\text{ Hz}$, 4 H), 2.35 (t, $^3J = 7.6\text{ Hz}$, 8 H), 1.50–1.40 (m, 8 H), 0.87 (t, $^3J = 7.4\text{ Hz}$, 12 H); $^{13}\text{C NMR}$ (125 MHz, CD_2Cl_2) δ 141.9, 131.8, 122.3, 92.8, 82.2, 35.9, 33.6, 29.6, 23.4, 13.9; IR (KBr) $\tilde{\nu} = 2954, 2926, 2867, 2153\text{ cm}^{-1}$; UV–vis (0.056 mg/mL in CH_2Cl_2) λ_{max} ($\log \epsilon$) = 336 (4.47), 286 (4.45) nm; FAB-MS m/z 628.2 (100, M^+); HRMS(FAB) calcd for $[\text{C}_{38}\text{H}_{44}\text{S}_4]^+$ 628.2326, found 628.2341. $\text{C}_{38}\text{H}_{44}\text{S}_4$ (628.23) calcd: C, 72.56; H, 7.05; S, 20.39. Found: C, 72.64; H, 7.10; S, 19.93.

X-ray Structure Analyses. The reflections were collected with a Bruker Smart CCD diffractometer at 200 K for **4(3)**, **4(5)**, **6**, **7(4)**,

7(5), **8(3)**, **8(4)**, and **24**, and a Bruker APEX diffractometer for **7(3)**, **8(5)**, **8(6)**, and **25**, both equipped with a sealed tube Mo $\text{K}\alpha$ radiation source and a graphite monochromator ($\lambda = 0.71073\text{ \AA}$). The data sets were collected at a temperature of 200 K for most of the structures; in the cases of **7(3)**, **8(5)**, and **25** the temperature was 100 K. Omega-scans of 0.3° were taken, covering a whole sphere in reciprocal space in each case. All intensities were corrected for Lorentz and polarization effects, and absorption corrections were applied using SADABS³¹ based on the Laue symmetry of the reciprocal space. The structures were solved by direct methods, the structural parameters of the non-hydrogen atoms were refined anisotropically according to a full-matrix least-squares technique against F^2 . Hydrogen atoms were treated by appropriate riding models, except for **8(5)** and **25** where they were refined isotropically and **8(6)** where they were treated in a mixed manner. Structure solution and refinement were carried out with the SHELXTL (5.10) software package.³² Crystallographic data and details of the data collection and the refinement procedure are given in Tables 3 and 4. CCDC-691838 (**4(3)**), -691839 (**4(5)**), -691840 (**6**), -691841 (**7(3)**), -691842 (**7(4)**), -691843 (**7(5)**), -691844 (**8(3)**), -691845 (**8(4)**), -691846 (**8(5)**), -691847 (**8(6)**), -691848 (**24**), and -691849 (**25**) contain the supplementary crystallographic data for this paper. Copies of the data can be obtained free of charge via www.ccdc.cam.ac.uk/conts/retrieving.html or on application to CCDC, 12 Union Road, Cambridge CB2 1EZ, U.K. [Fax: (int) +44-1223/336-033, E-mail: data_request@ccdc.cam.ac.uk], on quoting the deposition numbers. ORTEP drawings were obtained by Ortep-3 for Windows by Farrugia.³²

Acknowledgment. We are grateful to the Deutsche Forschungsgemeinschaft (DFG) and the Fonds der Chemischen Industrie for financial support. D.B.W. thanks the Studienstiftung des deutschen Volkes for a graduate fellowship. We thank Mrs. P. Krämer for typing the manuscript and A. Flatow for setting up the Supporting Information.

Supporting Information Available: Protocols for the preparation of diyne **19** and compounds **4–10** and **23–25**, as well as analytical data thereof. Crystal data (CIF files) for **4(3)**, **4(5)**, **6**, **7(3)–7(5)**, **8(3)–8(6)**, **24**, and **25**. This material is available free of charge via the Internet at <http://pubs.acs.org>.

JO801378P

(31) Sheldrick, G. M. *SADABS*; Bruker Analytical X-ray Division: Madison, WI, 1997.

(32) Sheldrick, G. M. *Acta Crystallogr. A* **2008**, *64*, 112–122.

(30) Eilbracht, P.; Acker, M.; Trotzauer, W. *Chem. Ber.* **1983**, *116*, 238–242.